Organic Process Research & Development **2009,** *13,* 1291–1300

Solvent Effects on the Crystallization and Preferential Nucleation of Carbamazepine Anhydrous Polymorphs: A Molecular Recognition Perspective

Ron C. Kelly[§] and Naír Rodríguez-Hornedo*

Department of Pharmaceutical Sciences, College of Pharmacy, University of Michigan, Ann Arbor, Michigan 48109, U.S.A.

Abstract:

This contribution reports the effects of molecular recognition events and solubility on the crystallization of carbamazepine (CBZ) polymorphs from organic solvents. Solvents were chosen on the basis of their hydrogen-bonding potential. Experiments were conducted to (1) measure solubilities and induction times, (2) monitor solution concentrations and solid phase compositions, and (3) identify intermolecular interactions between solvents and CBZ molecules. Primitive monoclinic, CBZ(M), and trigonal, CBZ(Trg), carbamazepine anhydrous polymorphs readily crystallized from the organic solvents. CBZ(Trg) is the metastable form at 25 °C with a solubility approximately 1.2 times that of CBZ(M). Results show that relative nucleation rates of CBZ polymorphs are dependent on the hydrogen-bonding nature of the solvent and are not dependent on solubility. Solvents that primarily accept hydrogen bonds (donor-to-acceptor ratio (d/a) = 0) preferentially crystallized CBZ(Trg), whereas solvents that accept and donate hydrogen bonds (d/a > 0.5) concomitantly crystallized CBZ(M) and CBZ(Trg). Evaluation of the crystal structures shows that specific interactions between acceptor solvents and the CBZ dimer led to the prevention of the molecular motif necessary for CBZ(M) nucleation. It is concluded that intermolecular interactions and specifically the hydrogen-bonding propensity of solvents with CBZ molecules have profound effects on the molecular self-assembly and selective crystallization of CBZ polymorphs.

Introduction

The effects of solvents on crystallization processes are important for understanding and developing methods for isolating crystal forms. When a drug compound exists in multiple crystal forms, developing a crystallization process that consistently yields the thermodynamically stable or desired crystal form reproducibly is not trivial. Control over the crystallization of solid forms is critical since each solid form will exhibit different physiochemical properties. Thermodynamic (solubility, temperature, solid−liquid interfacial tension, etc.) and kinetic factors (supersaturation, molecular mobility, nucleation rate, metastable zone width, etc.) as well as specific intermolecular interactions should be considered individually and collectively for selective crystallization of desired crystal forms.

Thermodynamics establishes the stability domains where multiple crystal forms exist. Once a metastable domain is encountered, kinetic pathways determine which form will crystallize.[1] This is the underlying concept in polymorph screening experiments where a diverse array of solvents is selected to generate all possible crystal forms.[2−4] Previous studies show that crystallization outcomes can be directly affected by the crystallizing solvent[1,5−9] and have been shown to be a result of solvent-dependent transformation kinetics.[3,10,11] In other words, crystallization from different solvents may yield different crystal forms where some of those crystal forms will be metastable and persist only because the kinetics of transformation is slower in some solvents than in others. While solvent diversity is important in screening for polymorphs, the appearance of crystal forms is not solely dependent on the solvent and may be a consequence of attaining critical concentrations.

Thermodynamic factors and the conditions in which the solvent may or may not affect crystallization outcomes has been considered.[12] While understanding the effects of solubility and

* Corresponding author. Telephone: 734-763-0101. Fax: 734-615-6162. E-mail: nrh@umich.edu.

§ Current address: Small Molecule Process and Product Development, Amgen, Inc., 1110 Veterans Blvd., South San Francisco, CA 94080.

(1) Miller, J. M., Blackburn, A. C., Macikenas, D. M., Collman, B. C., Rodríguez-Hornedo, N. Solvent Systems for Crystallization and Polymorph Selection. In *Solvent Systems and Their Selection in Pharmaceutics and Biopharmaceutics*; Augustins, P.; Brewster, M. E., Eds; AAPS Press: Arlington, VA, 2006.

(2) Miller, J. M.; Collman, B. M.; Greene, L. R.; Grant, D. J. W.; Blackburn, A. C. Identifying the stable polymorph early in the drug discovery development process. *Pharm. Dev. Technol.* **2005**, *10* (2), 291–297.

(3) Gu, C.; Young, V.; Grant, D. J. W. Polymorph Screening: Influence of Solvents on the Rate of Solvent-Mediated Polymorphic Transformation. *J. Pharm. Sci.* **2001**, *90* (11), 1878–1890.

(4) Hilfiker, R.; Berghausen, J.; Blatter, F.; Burkhard, A.; De Paul, S. M.; Freiermuth, B.; Geoffroy, A.; Hofmeier, U.; Marcolli, C.; Siebenhaar, B.; Szelagiewicz, M.; A., V.; von Raumer, M. Polymophism-Integrated approach from high-throughput screening to crystallization optimization. *J. Therm. Anal. Calorim.* **2003**, *73* (2), 429–440.

(5) Davey, R.; Blagden, N.; Righini, S.; Alison, H.; Ferrari, E. Nucleation Control in Solution Mediated Polymorphic Phase Transformations: The Case of 2,6-Dihydroxybenzoic Acid. *J. Phys. Chem. B* **2002**, *106* (8), 1954–1959.

(6) Davey, R. J., Solvent Effects in Crystallization Processes. In *Current Topics in Materials Science*; Kaldis, E., Ed.; North-Holland Publishing Company: 1982; pp 430−487.

(7) Khoshkhoo, S.; Anwar, J. Crystallization of Polymorphs: The Effect of Solvent. *J. Phys. D: Appl. Phys.* **1993**, *26* (8B), B90–B93.

(8) Blagden, N.; Davey, R. J.; Lieberman, H. F.; Williams, L.; Payne, R.; Roberts, R.; Rowe, R.; Docherty, R. Crystal chemistry and solvent effects in polymorphic systems: sulfathiazole. *J. Chem. Soc., Faraday Trans.* **1998**, *94* (8), 1035–1044.

(9) Bernstein, J. *Polymorphism in Molecular Crystals*; Oxford University Press; Oxford, 2002.

(10) Cardew, P. T.; Davey, R. J. The Kinetics of Solvent-Mediated Phase-Transformations. *Proc. R. Soc. London, Ser. A* **1985**, *398* (1815), 415–428.

(11) Davey, R. J.; Cardew, P. T.; McEwan, D.; Sadler, D. E. Rate Controlling Processes in Solvent-Mediated Phase Transformations. *J. Cryst. Growth* **1986**, *79* (1−3), 648–653.

(12) Threlfall, T. Crystallisation of Polymorphs: Thermodynamic Insight Into the Role of Solvent. *Org. Process Res. Dev.* **2000**, *4* (5), 384–390.

10.1021/op900133z CCC: $40.75
Published on Web 10/07/2009

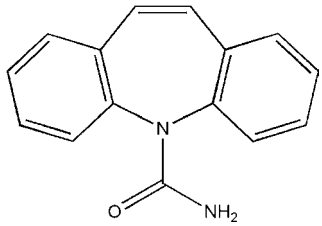

Figure 1. **Molecular structure of carbamazpine.**

solvent on crystallization events will improve the chances of isolating desired crystal forms, consideration must also be given to molecular recognition events. For instance, a metastable form that persists in a solvent may be the consequence of specific solute−solvent interactions that result in slower transformation kinetics.[1,3,7,8,13] Considering the delicate interplay that thermodynamic, kinetic, and molecular recognition factors have on crystallization outcomes,[14] it is not surprising that there is a lack of understanding in the factors that control crystallization events and the role that solvent plays as evident by literature reports detailing the difficulties to isolate crystal forms.[15−18] The main challenge is determining relationships between thermodynamics, kinetics, and specific intermolecular interactions that lead nuclei to form and grow. The work presented in this paper establishes relationships between solvents, solubility, and molecular recognition events for the selective crystallization of polymorphic forms.

Carbamazepine (CBZ) was chosen as the model compound for this research (Figure 1). Carbamazepine exists in at least four anhydrous forms: primitive monoclinic (CBZ(M), form III),[19] C-centered monoclinic (CBZ(IV), form IV),[20] trigonal (CBZ(Trg), form II),[21] and triclinic (CBZ(Trc), form I).[22] A dihydrate (CBZ(D)),[23] a monoacetonate (CBZ(Ace)),[24] and many multicomponent crystalline phases of CBZ[25,26] have also been identified. Among the anhydrous polymorphs, the primitive monoclinic polymorph (CBZ(M)) is the most stable form under ambient conditions. On the basis of studies conducted in our laboratory, CBZ(M) and CBZ(Trg) readily crystallize from organic solvents.

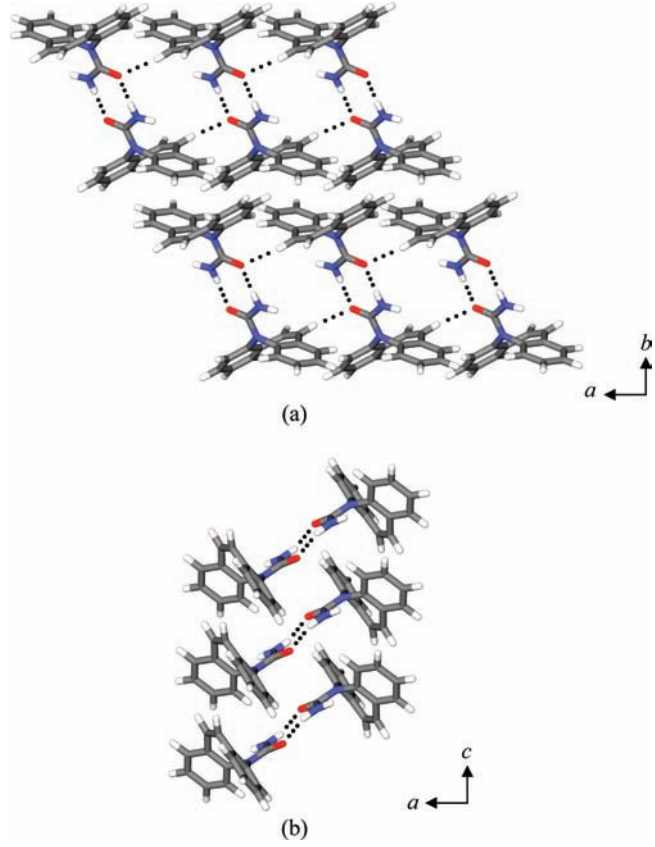

Figure 2. **Packing diagrams of (a) CBZ(M) and (b) CBZ(Trg). Some molecules not displayed for clarity.**

Carbamazepine polymorphism allows for the examination of how changing the crystallizing solvent and specific CBZ−solvent interactions alter nucleation behavior and molecular packing. By understanding the differences in intermolecular interactions and packing motifs of CBZ polymorphs (Figure 2), a rational approach for directing the nucleation of a given polymorph from organic solvents can be established.

The purpose of the work presented here was to investigate the effects of organic solvents on the nucleation of carbamazepine polymorphs, CBZ(M) and CBZ(Trg). The specific objectives of this research were (1) to determine the kinetic and molecular factors that govern the phase transformation and nucleation of CBZ polymorphs in organic solvents and (2) to understand the differences and similarities between the crystal

(13) Rodríguez-Hornedo, N.; Kelly, R. C.; Sinclair, B.; Miller, J. Crystallization: General Principles and Significance on Product Development. In *Encyclopedia of Pharmaceutical Technology*; Boylan, J. C.; Swarbrick, J., Eds.; Marcel Dekker Inc.: New York, 2006.
(14) Rodríguez-Spong, B.; Price, C. P.; Jayasankar, A.; Matzger, A. J.; Rodríguez-Hornedo, N. General principles of pharmaceutical solid polymorphsim: A supramolecular perspective. *Adv. Drug Delivery Rev.* **2004**, *56* (3), 241–274.
(15) Blagden, N.; Davey, R. J.; Rowe, R.; Roberts, R. Disappearing Polymorphs and the Role of Reaction Byproducts: The Case of Sulphathiazole. *Int. J. Pharm.* **1998**, *172* (1−2), 169–177.
(16) Dunitz, J. D.; Bernstein, J. Disappearing Polymorphs. *Acc. Chem. Res.* **1995**, *28* (4), 193–200.
(17) Bernstein, J.; Davey, R. J.; Henck, J. O. Concomitant Polymorphs. *Angew. Chem., Int. Ed.* **1999**, *38* (23), 3441–3461.
(18) Bernstein, J.; Henck, J. O. Disappearing and Reappearing Polymorphs: An Anathema to Crystal Engineering. *Cryst. Eng.* **1998**, *1* (2), 119–128.
(19) Himes, V.; Mighell, A.; De Camp, W. Structure of Carbamazepine: 5H-Dibenz[*b*,*f*]azepine-5-carboxamide. *Acta Crystallogr., Sect. B* **1981**, *B37* (12), 2242–2245.
(20) Lang, M. D.; Kampf, J. W.; Matzger, A. J. Form IV of Carbamazepine. *J. Pharm. Sci.* **2002**, *91* (4), 1186–1190.
(21) Lowes, M.; Caira, M.; Lotter, A.; Van Der Watt, J. Physicochemical Properties and X-ray Structural Studies of the Trigonal Polymorph of Carbamazepine. *J. Pharm. Sci.* **1987**, *76* (9), 744–752.
(22) Ceolin, R.; Toscani, S.; Gardette, M. F.; Agafonov, V. N.; Dzyabchenko, A. V.; Bachet, B. X-Ray Characterization of the Triclinic Polymorph of Carbamazepine. *J. Pharm. Sci.* **1997**, *86* (9), 1062–1065.
(23) Reck, G.; Dietz, G. The order-disorder structure of carbamazepine dihydrate: 5 H-dibenz [*b*,*f*] azepine-5-carboxamide dihydrate, $C_{15}H_{12}N_2O$. *Cryst. Res. Technol.* **1986**, *21* (11), 1463–1468.
(24) Terrence, C.; Sax, M.; Fromm, G.; Chang, C.; Yoo, C. Effect of Baclofen Enantiomorphs on the Spinal Trigeminal Nucleus and Steric Similarities of Carbamazepine. *Pharmacology* **1983**, *27* (2), 85–94.
(25) Fleischman, S.; Kuduva, S.; McMahon, J.; Moulton, B.; Walsh, R.; Rodríguez-Hornedo, N.; Zaworotko, M. Crystal Engineering of the Composition of Pharmaceutical Phases: Multiple-Component Crystalline Solids Involving Carbamazepine. *Cryst. Growth Des.* **2003**, *3* (6), 909–919.
(26) Childs, S. L.; Rodríguez-Hornedo, N.; Reddy, L. S.; Jayasankar, A.; Maheshwari, C.; McCausland, L.; Shipplett, R.; Stahly, B. C. Screening strategies based on solubility and solution composition generate pharmaceutically acceptable cocrystals of carbamazepine. *Cryst. Eng. Commun.* **2008**, *10* (7), 856–864.

structures that dictate polymorph appearance. Solvents studied were selected on the basis of their ability to interact through hydrogen bonding.

Materials and Methods

Materials. Anhydrous monoclinic carbamazepine, USP (CBZ(M), purity 99.8%) was purchased from Sigma Chemical Company (St. Louis, MO) and used as received. Carbamazepine was stored over anhydrous calcium sulfate at 4 °C. Solvents used in this study were purchased from Fisher Scientific (Springfield, NJ) and used as received.

X-ray Powder Diffraction (XRPD). Carbamazepine crystal identification was performed by XRPD. The powder patterns were obtained using a Scintag XDS2000 (Ecublens, Switzerland) diffractometer using Cu Kα radiation ($\lambda = 1.5418$ Å). X-ray scans were performed using 2θ values from 2° to 50° at a continuous scanning rate of 5°/min. Experimental powder patterns were compared to calculated powder patterns obtained from the solved crystal structures to identify and confirm polymorphic forms.

Scanning Electron Microscopy (SEM). Carbamazepine crystal morphology was examined by using a Hitachi scanning electron microscope (Tokyo, Japan). Samples were prepared by transferring carbamazepine crystals to a strip of double-sided carbon tape attached to a standard SEM mounting stub. The samples were coated with gold for 300 s using a Denton Vacuum Desk II gold coater (Moorestown, NJ). The microscope was operated with 15 kV beam current and a working distance of 15 mm.

Preparation of Carbamazepine Anhydrous Polymorphs. Carbamazepine triclinic was prepared by heating CBZ(M) isothermally in an oven at 140 °C for 4 h. The material was removed from the oven and allowed to cool to room temperature. The conversion of CBZ(M) to CBZ(Trc) was confirmed by XRPD.

Carbamazepine trigonal was prepared by making a supersaturated solution ($C/S_{CBZ(M)} = 2.0$ at 25 °C) with CBZ(M) as the starting material in ethyl acetate. The solution was heated to 50 °C with constant stirring. Once complete dissolution was achieved, the solution was crash cooled to 25 °C in an ice bath and allowed to crystallize for approximately 2 h. The crystals were filtered and dried under reduced pressure at room temperature for 45 min to remove any loosely bound solvent. Polymorphic form was confirmed by XRPD.

Equilibrium Solubility Measurement. The equilibrium solubility of CBZ(M) at 25 °C was measured in each solvent. An excess amount of CBZ(M) was suspended and stirred for 72 h. Temperature was controlled with water bath at 25.0 ± 0.1 °C. Samples were withdrawn using a 5-mL glass syringe and filtered through a Lida 0.45 μm PTFE filter (Kenosha, WI) enclosed in a stainless steel housing. Aliquots of the samples were weighed and diluted for UV analysis. Equilibration was reached when the concentration of two consecutive measurements at 48 and 72 h differed by no more than 2%. Carbamazepine concentration was determined using a Beckman DU-650 UV/vis spectrophotometer (Fullerton, CA) at a wavelength of 284.5 nm. X-ray powder diffraction was used to identify the solid phases at equilibrium.

The metastable solubilities of CBZ(Trg) and CBZ(Trc) were evaluated from the maximum of the concentration−time profiles during dissolution in undersaturated (initial $C/S_{CBZ(M)} = 0.80$ at 25 °C) 2-propanol solutions at 25 °C. Approximately 750 mg of CBZ(Trg) or CBZ(Trc) was suspended in 250 g of the 2-propanol solution in a jacketed beaker with constant agitation from an overhead stirrer (400 rpm). Solution- and solid-phase analysis followed the methods described above.

If the systems behave ideally, the rank order of CBZ polymorph solubility and solubility ratios are not solvent dependent. The solubility values were used to prepare supersaturated solutions for nucleation experiments.

Induction Time and Crystal Morphology. Induction times were measured in unstirred systems and small volumes (5 mL). Solutions (50 g) supersaturated with respect to CBZ(M) ($C/S_{CBZ(M)} = 2.0$ at 25 °C) were prepared by dissolving CBZ(M) in the desired solvent at 50 °C. The solutions were cooled by transferring to a jacketed beaker with the temperature controlled at 4.0 °C using a circulating water bath. An overhead stirrer was used to provide constant stirring (400 rpm). The jacketed beaker was drained to slow the cooling process when the solutions reached 30 °C to prevent overcooling and nucleation during transfer of solutions to smaller vials. Once the solution reached 25 °C, 5-mL aliquots were withdrawn and transferred to glass vials, and the glass vials were capped.

Induction times were measured by visual inspection using a Nikon Diaphot-TMD inverted microscope (Melville, NY) equipped with Nomarski objectives (10×). The time required for crystals to appear was noted as the induction time for each sample. Given that induction times are inversely proportional to nucleation rates, the relative nucleation rates were calculated by taking the inverse of the induction times and dividing each value by the fastest nucleation rate of CBZ(Trg) in order to normalize the values.

Crystal morphology was examined during induction time studies and recorded on the basis of a representative population in each sample. CBZ(M) and CBZ(Trg) crystallize in two distinct morphologies, prisms and needles, respectively. Crystal morphology was used to identify the forms present in the induction time and phase transformation experiments after the relationship between solid form and crystal morphology was confirmed by XRPD. Crystal morphologies were also examined by using scanning electron microscopy.

Phase Transformation in Solvents. Crystallization studies were performed at an initial supersaturation ($C/S_{CBZ(M)}$) of 2.0 at 25 °C, in stirred solutions, and in the absence of solid phase. Concentrations of CBZ in solutions were monitored along with phase composition of crystallized solids.

Solutions were prepared by dissolving CBZ(M) in 250 g of organic solvent by heating to 50 °C with constant stirring. The solutions were quickly cooled to 25 °C in an ice bath. The cooled supersaturated solution was added to a jacketed beaker with the temperature controlled at 25 °C and agitated with an overhead stirrer (400 rpm). Samples were withdrawn at known time intervals using a filtered syringe and diluted with the appropriate solvent. The concentration of carbamazepine was determined by UV/vis spectroscopy at a wavelength of 284.5 nm.

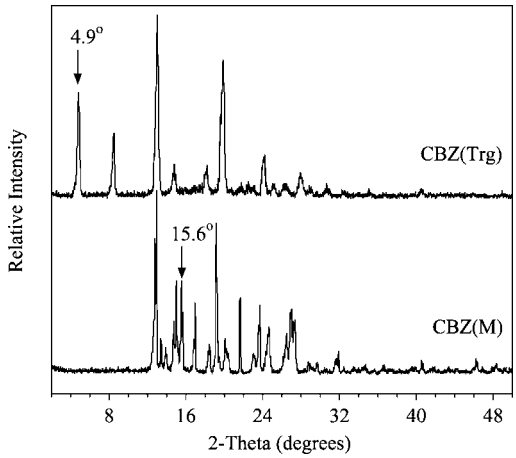

Figure 3. **Experimental XRPD patterns of CBZ(M) and CBZ(Trg).**

Solid phase composition during the experiments was analyzed by XRPD after removal of samples from the suspensions at determined time intervals. The collected sample was filtered and dried under reduced pressure to remove any loosely bound solvent. The percentage (w/w) of CBZ(M) and CBZ(Trg) was quantified by using a standard curve based on known quantities of CBZ(M) and CBZ(Trg). Samples were lightly ground to reduce the effects of preferred orientation. Diffraction peaks at 4.9° and 15.6° 2θ, corresponding to CBZ(Trg) and CBZ(M), respectively, were chosen to determine the polymorphic composition by comparing the integrated peak areas (Figure 3). Consecutive scans of the samples did not significantly affect the integrated peak areas. The detection limit was determined to be within 5%. The peak area ratio for CBZ(M) was calculated by:

$$\text{peak area ratio} = \frac{\text{peak area}(15.6^\circ)}{\text{peak area}(15.6^\circ) + \text{peak area}(4.9^\circ)} \quad (1)$$

Molecular Simulations. Molecular simulations were performed using Cerius^2 Molecular Simulations Package (Molecular Simulations, Inc., San Diego, CA) on an SGI Solid Impact 10000 workstation.

Morphology Prediction. The morphology module was used to calculate the crystal morphology using the attachment energy (AE) method.[27,28] The AE method is based on atom−atom interactions within the crystal. With the AE method, the crystal morphology is predicted by calculating the energy released when one layer of the molecular assembly is added to the growing crystal, which is proportional to the growth rate of the crystal face.[27,28] The force field used (cff91_950_1.01) was evaluated by comparing the changes in lattice parameters during the molecular minimization of an unconstrained unit cell. The force field was deemed appropriate if the lattice parameters changed less than 5% after minimization.

Morphology calculations were compared to the morphology of crystals grown from solution in order to determine molecular packing within the crystal planes.

Results

Solubility of Carbamazepine Anhydrous Polymorphs. The equilibrium solubility of CBZ(M) was measured in order to accurately calculate supersaturation and allow for meaningful comparisons of the solvent effects on CBZ crystallization. Solvents were chosen on the basis of their ability to accept or donate hydrogen bonds as described by Marcus, et al.[29] and are listed in Table 1. Solubility values for CBZ(M) are also presented in Table 1. Results also show that CBZ(Trg) and CBZ(Trc) are 1.18 and 1.25 times more soluble than CBZ(M) at 25 °C (Figure 4).

The solubility of a compound is related to the strength of the solute−solvent interactions. By fitting the linear free energy equation (eq 2)

$$\log s = a + b \times \delta^2 + c \times \Sigma\alpha + d \times \Sigma\beta + e \times \pi^* \quad (2)$$

to the experimental solubility of CBZ(M) and using the reported solvent parameters,[29,30] the following relationship was obtained (eq 3):

$$\log s = -3.86 - 0.011\delta^2 + 2.15\Sigma\alpha - 1.16\Sigma\beta + 4.68\pi^*$$
$$r^2 = 0.942 \quad (3)$$

where s is the solubility (mole fraction), δ is the solubility parameter corresponding to the square root of the cohesive energy density, $\Sigma\alpha$ is the hydrogen-bond-donor propensity (HBD), $\Sigma\beta$ is the hydrogen-bond-acceptor propensity (HBA), π^* is the polarity/polarizability parameter, and a, b, c, d, and e are coefficients that are determined from linear regression. The quantities for hydrogen-bond ability and polarity/polarizability reported by Marcus[29] and used in our calculations are shown in Table 1. These are solvatochromic properties that were spectroscopically determined with suitable indicators. Solubility parameter values, δ, reported by Hoy[30] based on solvent vapor pressure measurements to calculate heats of vaporization were used. The coefficients for δ and $\Sigma\beta$ were found to be negative, indicating that CBZ(M) solubility is inversely proportional to both δ and $\Sigma\beta$. However, the coefficients for $\Sigma\alpha$ and π^* were found to be positive, suggesting that CBZ(M) solubility is directly proportional to $\Sigma\alpha$ and π^*. Given that π^* has the largest coefficient, CBZ(M) solubility has the strongest dependence on solvent polarizability (Figure 5).

Effects of Solvents on CBZ Induction Time and Crystal Morphology. The relative nucleation rates were evaluated with regard to solubility and solvent properties to determine the factors that dictate CBZ nucleation outcomes. Induction times are defined as the time required for nuclei to grow into visible crystals, and are inversely proportional to nucleation rates.[31,32]

(27) Hartman, P.; Bennema, P. The attachment energy as a habit controlling factor: I. Theoretical considerations. *J. Cryst. Growth* **1980**, *49* (1), 145–149.
(28) Berkovitch-Yellin, Z. Toward an ab Initio Derivation of Crystal Morphology. *J. Am. Chem. Soc.* **1985**, *107* (26), 8239–8253.
(29) Marcus, Y. The Properties of Organic Liquids That Are Relevant to Their Use as Solvating Solvents. *Chem. Soc. Rev.* **1993**, *22* (6), 409–416.
(30) Hoy, K. L. New values of the solubility parameters from vapor pressure data. *J. Paint Technol.* **1970**, *42* (541), 76–118.

Table 1. **CBZ(M) equilibrium solubility ($n = 3$) and induction times ($C/S = 2.0$, $n = 10$, unstirred) in organic solvents at 25 °C**

solvent	CBZ(M) solubility mg/g, avg (SD)	induction time, min avg (SD), $t_{ind}^{-1} \propto J$		$\Sigma\alpha^{a29}$ (HBD)	$\Sigma\beta^{b29}$ (HBA)	π^{*c29}	δ^{d30} $(cal/cm^3)^{1/2}$
		CBZ(Trg)	CBZ(M)				
ethyl propionate	7.12 (0.01)	0.5[e]	2000 (1000)	0	0.36	0.58	8.77
ethyl acetate	11.63 (0.02)	0.5[e]	300 (20)	0	0.45	0.55	8.91
methyl acetate	19.32 (0.03)	0.5[e]	100 (30)	0	0.42	0.60	9.46
2-butanone	27.80 (0.05)	0.5[e]	50 (4)	0.06	0.48	0.67	9.45
chloroform	123.44 (0.06)	2 (1)	20 (12)	0.20	0.10	0.58	9.16
methylene chloride	154.45 (0.38)	0.5[e]	20 (9)	0.13	0.10	0.82	9.88
acetonitrile	48.70 (0.23)	3 (1)	3 (1)	0.19	0.40	0.75	12.11
2-propanol	11.68 (0.48)	5 (3)	5 (3)	0.76	0.84	0.48	11.44
1-propanol	22.48 (0.01)	4 (2)	4 (2)	0.84	0.90	0.52	12.18
ethanol	32.21 (0.02)	3 (1)	3 (1)	0.86	0.75	0.54	12.78
methanol	95.93 (0.04)	2 (1)	2 (1)	0.98	0.66	0.60	14.50
hexanes	0.04 (0.01)	2 (1)	2 (1)	0	0	0	7.27
cyclohexane	0.07 (0.01)	12 (8)	12 (8)	0	0	0	8.19

[a] Hydrogen bond donor propensity. [b] Hydrogen bond acceptor propensity. [c] Polarity/polarizability. [d] Solubility parameter values are similar to those reported by Hansen (±2%): Hansen, C. Hansen Solubility Parameters: A User's Handbook; CRC Press: Boca Raton, FL, 2000. [e] Experimental error is ± 15%.

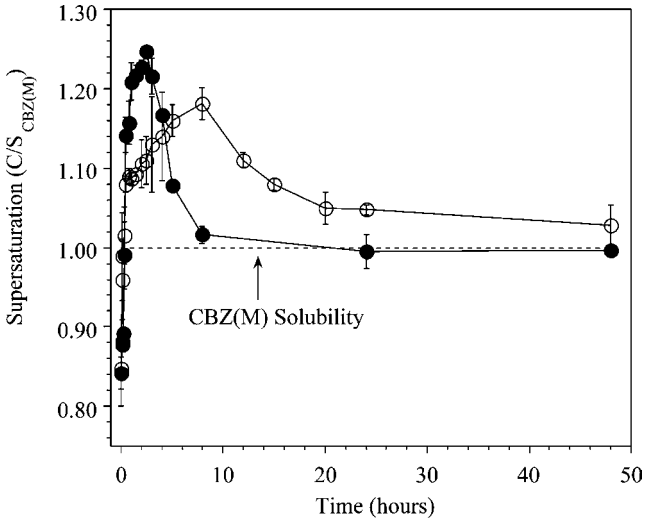

Figure 4. **Concentration−time profile in 2-propanol during the dissolution of (○) CBZ(Trg) and (●) CBZ(Trc) at 25 °C. Error bars represent standard deviation.**

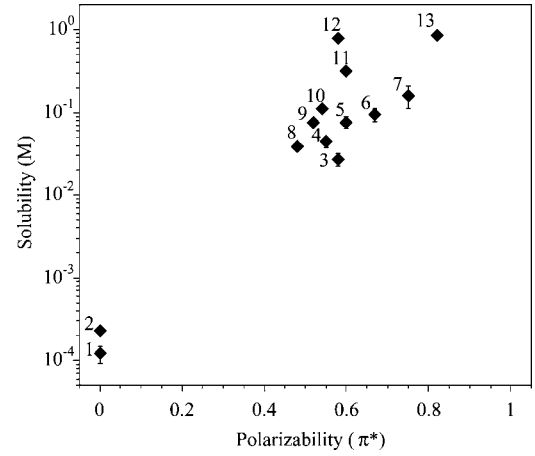

Figure 5. **CBZ(M) solubility as a function of solvent polarity. Error bars represent standard deviation. (1) cyclohexane, (2) hexanes, (3) ethyl propionate, (4) ethyl acetate, (5) methyl acetate, (6) 2-butanone, (7) acetonitrile, (8) 2-propanol, (9) 1-propanol, (10) ethanol, (11) methanol, (12) chloroform, (13) methylene chloride.**

Relative nucleation rates ($(t_{ind,x}^{-1})/(t_{ind,CBZ(Trg)}^{-1})$) were calculated from the measured induction times for both CBZ(M) and CBZ(Trg). CBZ(Trg) was used as the reference in evaluating CBZ nucleation since CBZ(Trg) had the fastest induction time, 0.5 min, (Table 1).

Induction time results show that CBZ(M) and CBZ(Trg) crystallized concomitantly or CBZ(Trg) crystallized preferentially (Table 1), depending on the solvent. The induction time for concomitant crystallization ranges between 3 and 12 min, whereas for preferential CBZ(Trg) nucleation the induction time is 0.5−2 min with the subsequent nucleation of CBZ(M) at 20−2000 min.

Nucleation events are a consequence of thermodynamic, kinetic, and molecular recognition events. In turn, kinetic and molecular recognition events can be directly affected by the solubility and specific solvent properties (polarizability, solubility parameter, or hydrogen bond propensity).

The influence of solubility on the nucleation rate can be explained by the classical nucleation theory[32] in which the rate for nucleation of spherical clusters is given by

$$J = N_0 \nu \exp\left(\frac{-16\pi v^2 \gamma_{12}^3}{3k^3T^3\left(\ln\left(\frac{C}{S}\right)\right)^2}\right) \qquad (4)$$

where J is the number of nuclei formed per unit time per unit volume, N_0 is the number of molecules of the crystallizing phase in a unit volume, ν is the frequency of molecular transport at the nucleus−liquid interface, v is the molecular volume of the crystallizing solute, and γ_{12} is the interfacial energy per unit area between the crystallization medium, 1, and the nucleating cluster, 2, T is the absolute temperature in Kelvin, k is the Boltzmann constant, and C/S is the supersaturation. The classical nucleation equation predicts that under constant supersaturation

(31) Myerson, A. S. *Handbook of Industrial Crystallization*, 2nd ed.; Butterworth-Heinemann: Oxford, 2002.
(32) Mullin, J. W. *Crystallization.* 4th ed.; Butterworth-Heinemann; Oxford, 2001.

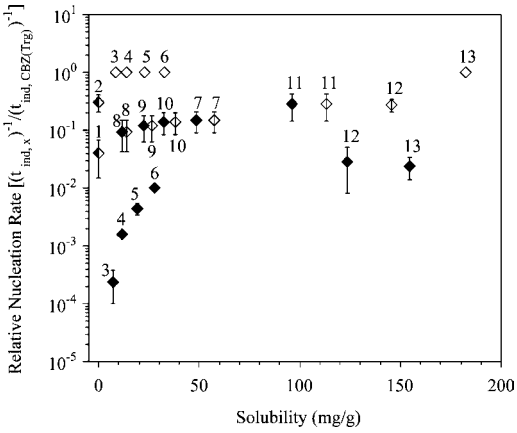

Figure 6. **CBZ relative nucleation rate as a function of solubility at 25 °C and $C/S_{CBZ(M)} = 2.0$. (open symbols) CBZ(Trg), (solid symbols) CBZ(M), (half-solid half-open symbols) overlay of open and closed symbols. (1) cyclohexane, (2) hexanes, (3) ethyl propionate, (4) ethyl acetate, (5) methyl acetate, (6) 2-butanone, (7) acetonitrile, (8) 2-propanol, (9) 1-propanol, (10) ethanol, (11) methanol, (12) chloroform, (13) methylene chloride. Error bars represent standard deviation.**

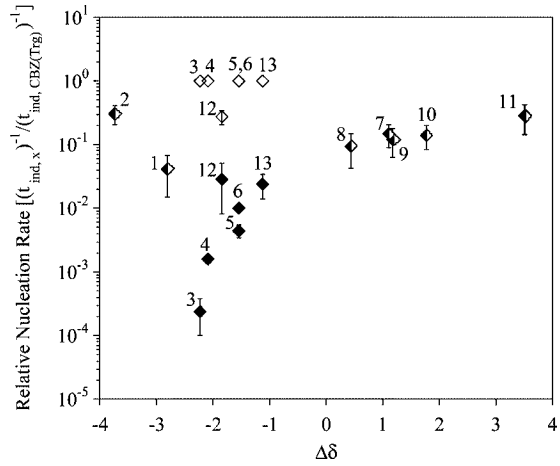

Figure 7. **CBZ relative nucleation rate as a function of the difference between CBZ and solvent-solubility parameters ($\Delta\delta$) at 25 °C and $C/S_{CBZ(M)} = 2.0$. (open symbols) CBZ(Trg), (solid symbols) CBZ(M), (half-solid half-open symbols) overlay of open and closed symbols. (1) cyclohexane, (2) hexanes, (3) ethyl propionate, (4) ethyl acetate, (5) methyl acetate, (6) 2-butanone, (7) acetonitrile, (8) 2-propanol, (9) 1-propanol, (10) ethanol, (11) methanol, (12) chloroform, (13) methylene chloride. Error bars represent standard deviation.**

the rate of nucleation is faster in systems with higher solubilities. In addition, polymorphs with similar solubilities are expected to favor concomitant crystallization. Increases in solubility result in an increase in the pre-exponential factor, $N_0\nu$, and the probability of intermolecular collisions. When changes in solvent lead to increases in solubility, the interfacial energy decreases since the affinity between crystallizing medium and crystal increases.

Increase in CBZ nucleation rate with increasing solubility as predicted by eq 4 was not experimentally observed (Figure 6). Even though concomitant crystallization is observed in hexanes, cyclohexane, 1-propanol, 2-propanol, ethanol, methanol, and acetonitrile, CBZ(M) nucleation rate is approximately 2−4 orders of magnitude slower than CBZ(Trg) in other solvents: ethyl propionate, ethyl acetate, methyl acetate, 2-butanone, chloroform, and methylene chloride. When comparing alcohols to ester solvents, CBZ(M) nucleation rate is 2−3 orders of magnitude greater in alcohols than esters at similar solubilities (Table 1, Figure 6).

The nucleation rate equation does not accurately predict CBZ nucleation behavior because it does not capture the specific solute−solvent interactions that may control nucleation outcomes. This suggests that there is a balance between the kinetic and molecular association events for CBZ nucleation. Therefore, molecular properties of the solvents and intermolecular interactions between the solvents and CBZ were examined, such as solubility parameter, polarizability, and hydrogen-bonding propensity.

Results show that solvents with solubility parameters in the range of 11.4−14.5 $(cal/cm^3)^{1/2}$ led to concomitant crystallization of CBZ(Trg) and CBZ(M) (Table 1). Concomitant crystallization was also observed in solvents with solubility parameters less than 8.2 $(cal/cm^3)^{1/2}$. Solvents with solubility parameters between 8.7 and 9.9 $(cal/cm^3)^{1/2}$ led to preferential crystallization of CBZ(Trg) (Table 1). The solubility parameter for CBZ has been calculated to be approximately 12.6 $(cal/cm^3)^{1/2}$.[33] With the exceptions of cyclohexane and hexanes, evaluating CBZ nucleation in terms of the difference in solubility parameters ($\Delta\delta$) between the solvent and CBZ shows a trend where solvents with negative $\Delta\delta$ values led to preferential CBZ(Trg) nucleation, while solvents with positive $\Delta\delta$ led to concomitant crystallization of CBZ(Trg) and CBZ(M) (Figure 7).

It would appear that the solubility parameter can be used to predict CBZ nucleation. However, it should be noted that the solubility parameter captures the dispersion, polar, and hydrogen-bonding forces that constitute the cohesive energy necessary for intermolecular interactions.[34−36] The solubility parameter (δ) is represented by the following equation:

$$\delta = \sqrt{\delta_d^2 + \delta_p^2 + \delta_h^2} \qquad (5)$$

where δ_d, δ_p, δ_h, are the partial solubility parameters for the dispersion, polar, and hydrogen-bond forces, respectively. Each individual force was evaluated separately to determine its contribution towards CBZ nucleation outcomes. Dispersion forces were not directly investigated since they are generally weaker than polar and hydrogen-bond interactions and are not expected to have a significant impact on CBZ nucleation. While solvent polarizability has a strong influence on CBZ solubility (Figure 5), there was no correlation between solvent polarizability and nucleation (Figure 8). Therefore, CBZ nucleation was examined in relation to the hydrogen-bonding propensity of the solvent.

The solvents that possessed the greatest ability to concomitantly crystallize CBZ(M) and CBZ(Trg) were

(33) Subrahmanyam, C. V. S.; Sarasija, S. Solubility Behaviour of Carbamazepine in Binary Solvents: Extended Hildebrand Solubility Approach to Obtain Solubility and Other Parameters. *Pharmazie* **1997**, *52* (12), 939–942.
(34) Fedors, R. F. Method for Estimating Both Solubility Parameters and Molar Volumes of Liquids. *Polym. Eng. Sci.* **1974**, *14* (2), 147–154.
(35) van Krevelen, D.; Hoftyzer, P. *Properties of Polymers, Their Estimation and Correlation with Chemical Structure*, 2nd ed.; Elsevier: Amsterdam, 1976.
(36) Greenhalgh, D. J.; Williams, A. C.; Timmins, P.; York, P. Solubility Parameters as Predictors of Miscibility in Solid Dispersions. *J. Pharm. Sci.* **1999**, *88* (11), 1182–1190.

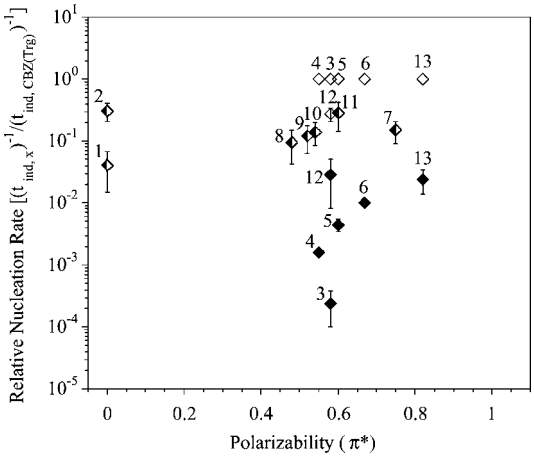

Figure 8. **CBZ relative nucleation rates a function of solvent polarity at 25 °C and $C/S_{CBZ(M)} = 2.0$. (open symbols) CBZ(Trg), (solid symbols) CBZ(M), (half-solid half-open symbols) overlay of open and closed symbols. (1) cyclohexane, (2) hexanes, (3) ethyl propionate, (4) ethyl acetate, (5) methyl acetate, (6) 2-butanone, (7) acetonitrile, (8) 2-propanol, (9) 1-propanol, (10) ethanol, (11) methanol, (12) chloroform, (13) methylene chloride. Error bars represent standard deviation.**

cyclohexane, hexanes, acetonitrile, 2-propanol, 1-propanol, ethanol, and methanol (Figure 9a). With the exception of cyclohexane and hexanes, which have no hydrogen-bond potential, these solvents interact through accepting and donating hydrogen bonds (Table 1).

The solvents that exhibited the most discriminating power for inhibiting CBZ(M) nucleation and preferentially nucleating CBZ(Trg) were ethyl propionate, ethyl acetate, methyl acetate, 2-butanone, chloroform, and methylene chloride (Figure 9b). These solvents primarily interact by accepting hydrogen bonds with the exception of chloroform and methylene chloride. It has been shown that chlorinated solvents possess a stronger ability to accept than donate hydrogen bonds due to the additive acceptor propensity of each chlorine atom,[37] even though this is not reflected in the overall hydrogen-bond propensities, $\Sigma\alpha$ and $\Sigma\beta$.

The balance between hydrogen bond donors to acceptors of the solvents is reflected by the ratio of hydrogen-bond propensities, HBD/HBA. With the exceptions of cyclohexane, hexanes, chloroform, and methylene chloride, Figure 10 shows that concomitant crystallization of CBZ(Trg) and CBZ(M) occurs as the HBD/HBA ratio increases. Solvents with only hydrogen-bond-acceptor propensity, HBD/HBA of 0, led to the preferential crystallization of CBZ(Trg).

The CBZ(M) nucleation rate is 2−4 orders of magnitude slower than CBZ(Trg) in acceptor solvents: ethyl propionate, ethyl acetate, methyl acetate, and 2-butanone. In this class of solvents, the CBZ(M) nucleation rate is proportional to the solubility (Table 1, Figures 6−10). The nucleation of CBZ(M) in these solvents indicates the beginning stages of the metastable CBZ(Trg) to stable CBZ(M) transformation. The transformation rate will depend on the absolute and relative magnitudes of the solubilities of the crystal phases involved, and would be

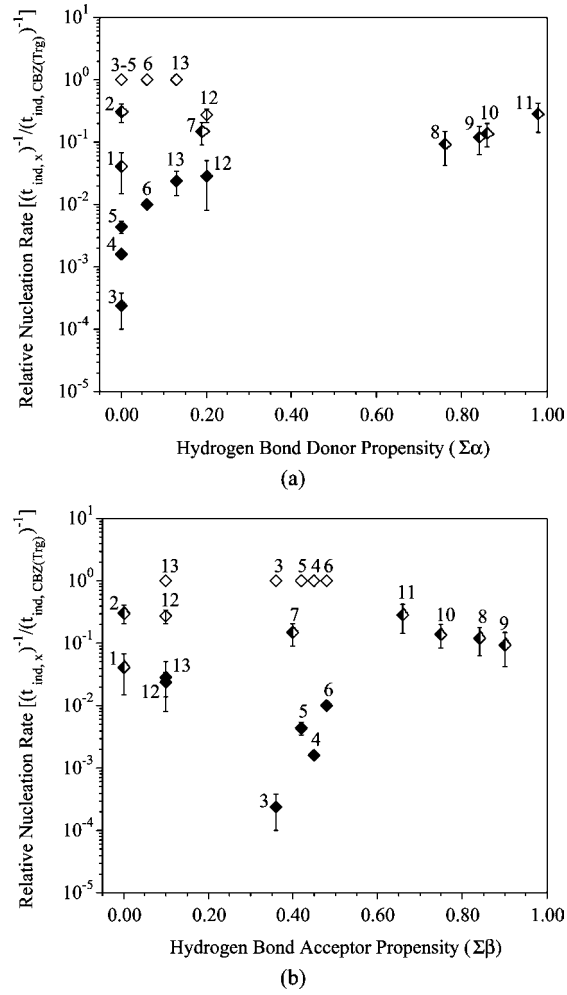

Figure 9. **Relationship between CBZ nucleation rate and (a) hydrogen-bond-donor and (b) hydrogen-bond-acceptor propensity at 25 °C and $C/S_{CBZ(M)} = 2.0$. (open symbols) CBZ(Trg), (solid symbols) CBZ(M), (half-solid half-open symbols) overlay of open and closed symbols. (1) cyclohexane, (2) hexanes, (3) ethyl propionate, (4) ethyl acetate, (5) methyl acetate, (6) 2-butanone, (7) acetonitrile, (8) 2-propanol, (9) 1-propanol, (10) ethanol, (11) methanol, (12) chloroform, (13) methylene chloride. Error bars represent standard deviation.**

expected to decrease as the solubility decreases.[38] However, the significance of solute−solvent interactions on transformation rates cannot be neglected. Intermolecular interactions also have significant effects on transformation rates and should be thoroughly considered when evaluating nucleation outcomes.

Crystal morphologies of CBZ(Trg) and CBZ(M) were solvent independent, suggesting that there is no preferential interaction between solvent and specific crystal faces. CBZ(Trg) grows predominantly along the *c*-axis as needles, whereas CBZ(M) grows along each crystallographic direction (*a*, *b*, and *c*) as prisms. The experimental crystal morphologies are in good agreement with the predictions based on attachment energy calculations (Figures 11 and 12).

Phase Transformation in Solvents. The supersaturation profiles as a result of nucleation and solvent-mediated transformation of CBZ polymorphs in 2-propanol and ethyl acetate

(37) Abraham, M. H.; Enomoto, K.; Clarke, E. D.; Sexton, G. Hydrogen Bond Basicity of the Chlorogroup; Hexachlorocyclohexanes as Strong Hydrogen Bond Bases. *J. Org. Chem.* **2002**, *67* (14), 4782–4786.

(38) Cardew, P. T.; Davey, R. J. Kinetic Factors in the Appearance and Transformation of Metastable Phases. *Institute of Chemical Engineers, North Western Branch, Symposium Papers No. 2;* 1982.

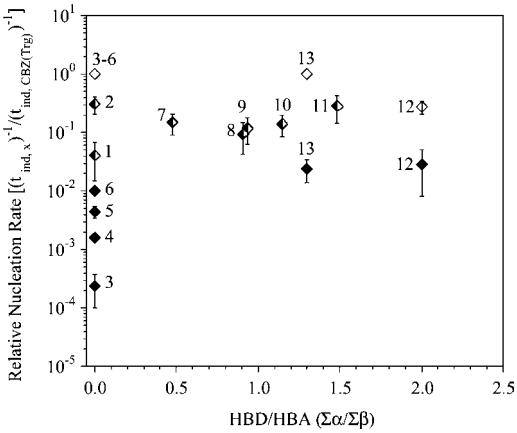

Figure 10. **CBZ nucleation as a function of HBD/HBA at 25 °C and $C/S_{CBZ(M)}$ = 2.0. (open symbols) CBZ(Trg), (solid symbols) CBZ(M), (half-solid half-open symbols) overlay of open and closed symbols. (1) cyclohexane, (2) hexanes, (3) ethyl propionate, (4) ethyl acetate, (5) methyl acetate, (6) 2-butanone, (7) acetonitrile, (8) 2-propanol, (9) 1-propanol, (10) ethanol, (11) methanol, (12) chloroform, (13) methylene chloride. Error bars represent standard deviation.**

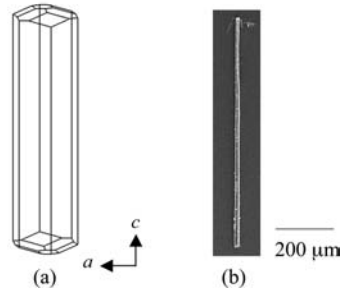

Figure 11. **(a) Calculated crystal morphology of CBZ(Trg) (Attachment Energy Model, Force field: cff91_950_1.01) and (b) experimental crystal morphology of CBZ(Trg) grown from ethyl acetate at 25 °C and $C/S_{CBZ(M)}$ = 2.0. Harvested 24 h after nucleation.**

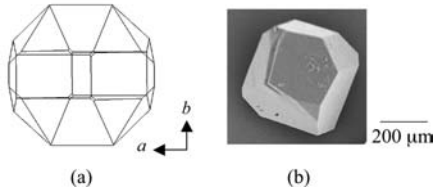

Figure 12. **(a) Calculated crystal morphology of CBZ(M) (Attachment Energy Model, Force field: cff91_950_1.01) and (b) Experimental crystal morphology of CBZ(M) grown from 2-propanol at 25 °C and $C/S_{CBZ(M)}$ = 2.0. Harvested 24 h after nucleation.**

are shown in Figure 13. 2-Propanol and ethyl acetate were chosen as model solvents since CBZ(M) solubility at 25 °C is not significantly different in the two solvents (0.04 M), and the induction time studies in unstirred systems (5 mL) showed different crystallization behavior; 2-propanol led to concomitant crystallization while ethyl acetate led to preferential crystallization of CBZ(Trg). These results under stirred conditions and larger mass (250 g of solvent) are in agreement with the induction time studies under unstirred conditions and smaller volumes (5 mL) and show that the crystallization process is solvent dependent.

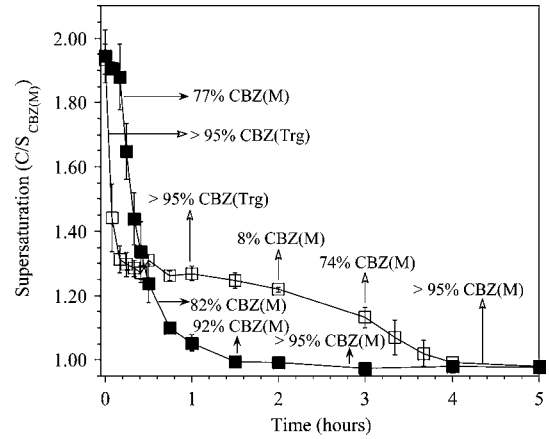

Figure 13. **Carbamazepine supersaturation-time profile and percent solid phase composition in (■) 2-propanol and (□) ethyl acetate at 25 °C and an initial $C/S_{CBZ(M)}$ = 2.0. Error bars represent standard deviation. Agitation provided via overhead stirrer (400 rpm).**

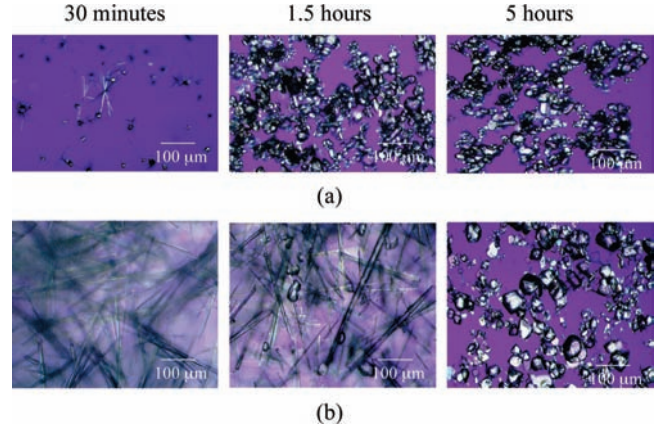

Figure 14. **Photomicrographs of CBZ solvent-mediated phase transformation in (a) 2-propanol and (b) ethyl acetate at 25 °C and an initial $C/S_{CBZ(M)}$ = 2.0.**

The rate of transformation to CBZ(M) is faster in 2-propanol than in ethyl acetate. XRPD analysis of the solid phase in 2-propanol shows that after 20 min 77% of the solid phase is CBZ(M) and the supersaturation profile reaches a C/S of 1.0 after 1.5 h when at least 92% of the solid phase is CBZ(M). In ethyl acetate CBZ(Trg) is preferentially crystallized with more than 95% CBZ(Trg) present as the solid phase in the initial stages of the transformation. The supersaturation profile decreases and sustains a steady concentration at a $C/S_{CBZ(M)}$ of approximately 1.25, which is close to the solubility of CBZ(Trg) (CBZ(Trg)/CBZ(M) solubility ratio at 25 °C = 1.2). This steady-state is maintained until a large fraction of the solid phase is transformed to CBZ(M), approximately 74%, where CBZ(M) grows at the expense of CBZ(Trg) dissolution. The supersaturation profile reaches a $C/S_{CBZ(M)}$ of 1.0 after 4 h, where more than 95% of the solid phase is CBZ(M). Figure 14 shows photomicrographs depicting the difference in crystallization behavior between the two solvents.

Mathematical simulations based on models developed by Cardew and Davey[10] were employed to discern between dissolution or growth limited crystallization process. Desupersaturation profiles were analyzed in terms of dissolution (k_d)

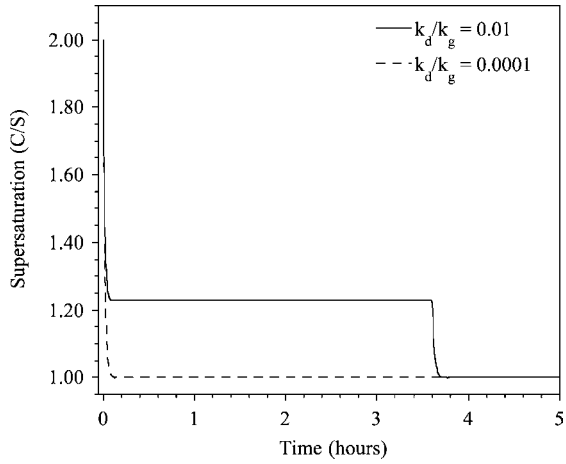

Figure 15. **Mathematical simulation of the supersaturation time profiles as a function of the relative rates of dissolution and crystallization during a solution-mediated transformation. Generated from a kinetic model developed by Cardew and Davey[10,11] with constants $L_{Mi} = 100\ \mu m$, $L_{Sf} = 300\ \mu m$, $\sigma_i = 2.0$, $\sigma_{SM} = 1.2$.**

and growth (k_g) rate constants[5,11] according to the first order equations below:

$$\frac{dL_M}{dt} = -k_d(\sigma_{SM} - \sigma_S) \tag{6}$$

and

$$\frac{dL_S}{dt} = k_g\sigma_S \tag{7}$$

where the subscripts S and M represent the stable and metastable forms, L is the crystal size, σ_S is the relative supersaturation with respect to the stable phase, $((C - S)/(S))$, and k_d and k_g are the rate constants for the dissolution and growth processes. The term σ_{SM} is defined as:

$$\sigma_{SM} = \frac{(S_M - S_S)}{S_S} \tag{8}$$

Based on these equations, the mass balance equation during a solution-mediated transformation is:

$$\sigma = \sigma_i - (\sigma_i - \sigma_{SM})\left(\frac{L_M}{L_{Mi}}\right)^3 - \sigma_i\left(\frac{L_S}{L_{Sf}}\right)^3 \tag{9}$$

where σ_i is the supersaturation that would exist if all the solid phase dissolved in solution and L_{Mi} and L_{Sf} are the initial and final sizes of the metastable and stable crystals, respectively. The above equations can be solved simultaneously to simulate the supersaturation as a function of time during a solvent-mediated transformation.

A calculated supersaturation profile with growth and dissolution-limited regimes is shown in Figure 15. This model describes processes where solid phase is present in the system, and here it is applied to systems after the onset of instantaneous nucleation, as observed in the phase transformation studies presented in this work. The model is presented in terms of C/S instead of $(C - S)/S$ and σ_{SM} is defined as S_M/S_S in order to be consistent with the experimental data. The values for L_{Mi} (100 μm) and L_{Sf} (300 μm) are based on the average initial CBZ(Trg) and final CBZ(M) sizes measured by optical microscopy during crystallization experiments. The initial crystal size was obtained approximately ten minutes after crystallization began and was based on a representative population of the crystals. Final crystal sizes were obtained approximately 24 h after the start of the crystallization study and were also based on a representative population of crystals.

From the initial supersaturation the nucleation is accompanied by a decrease in concentration: when $k_d/k_g = 0.01$ a decrease in concentration will approach the solubility of the metastable phase and the elevated concentration is maintained until the stable phase nucleates. In this process, the phase transformation is rate-limited by the nucleation and growth of the stable crystal form. On the other hand, if both forms nucleate concomitantly and $k_d/k_g = 0.0001$, the decline in concentration will approach the solubility of the stable phase and will be rate-limited by the extent of nucleation and dissolution of the metastable phase.

Comparing the mathematical simulations (Figure 15) to the experimental results (Figure 13), the rate-limiting step for CBZ crystallization and phase transformation is dependent on the solvent. In 2-propanol the phase transformation is rate-limited by the nucleation and dissolution of the metastable CBZ(Trg). In contrast, the rate-limiting step in ethyl acetate is the nucleation and growth of the stable CBZ(M).

Discussion

The results of this research show that under constant initial supersaturation the nucleation and phase transformation of CBZ polymorphs are dependent on the hydrogen-bond propensity of the solvent. The difference in CBZ nucleation behavior may be attributed to the specific CBZ−solvent interactions. The discussion that follows examines the role that three factors have on directing CBZ nucleation events: (1) balance between hydrogen bond donors to acceptors, (2) differences in CBZ crystal structures, and (3) specific CBZ−solvent interactions.

The balance between hydrogen bond donors to acceptors has a significant role in directing CBZ nucleation events. Results show that solvents with a hydrogen bond donor to acceptor ratio $(d/a) = 0$ (hydrogen bond acceptor) crystallized the metastable CBZ(Trg) preferentially, while solvents with a $d/a \geq 0.5$ (hydrogen bond acceptor and donator) crystallized CBZ(Trg) and CBZ(M) concomitantly. Clearly, the local chemical environment of the solute−solvent system influences the nucleation outcomes. While the balance between hydrogen bond donors to acceptors of the crystallizing solvents gave some insight to CBZ crystallization behavior, the role of hydrogen-bond propensity in directing nucleation outcomes may be better understood by establishing a relationship between nucleation and the crystal structures of both CBZ(M) and CBZ(Trg).

The crystal structures of both CBZ(M) and CBZ(Trg) are characterized by centrosymmetric dimers formed by hydrogen bonding between carboxamide groups that stack through $\pi-\pi$ interactions (Figure 2). Although the CBZ dimer formation and types of interactions are similar in the two structures, the packing and orientation of the molecules are different, which may contribute to the observed differences in nucleation behavior.

In CBZ(M), the centrosymmetric dimers are present mainly along the *b*-axis with partial overlap between CBZ molecules that stack through $\pi-\pi$ interactions along the *a*- and *c*-axes (Figure 2a). The CBZ dimers are linked through close C−H···O interactions involving a vinylic hydrogen on the azepine ring to the oxygen of the carboxamide group in the next growth layer to form chains of CBZ dimers along each crystallographic direction.[20,39] In addition, the C−H···O interaction aids in stabilizing the close packing (0.07 Å) between the carboxamide planes within the CBZ(M) structure.[19,20,39] The molecular arrangement of the CBZ molecules in the CBZ(M) crystal structure contributes to the herringbone motif and the close packing of the molecules, which results in the prismatic crystal morphology (Figure 12).

In comparison, the CBZ(Trg) crystal structure is due to the presence of hydrogen bonding and stacking of CBZ dimers through $\pi-\pi$ interactions primarily along the *c*-direction (major axis of growth),[21] which leads to the needle morphology (Figure 11). The C−H···O interaction forms chains of CBZ dimers in the crystal faces growing perpendicular to the *b*-crystallographic direction. This interaction does not form along the major growth axis (*c*-axis), which may contribute to the lack of close facial aromatic stacking within the CBZ(Trg) crystal structure (Figure 2b).[20,39] The C−H···O interaction is not needed to stabilize the CBZ(Trg) molecular motif.

While CH···O hydrogen bonds are typically weak interactions, they have been documented to serve as important secondary interactions and in many instances play dominant roles in determining crystal packing and molecular conformation,[40−42] and is relevant to CBZ crystal structures.[20,39] Since the CH···O interaction is critical in stabilizing the CBZ(M) structure, a solvent that primarily accepts hydrogen bonds can disrupt the CH···O interaction, destabilize the crystal structure, and prevent the stacking pattern and molecular motif necessary for CBZ(M) nucleation. This interaction is less likely to affect CBZ(Trg) nucleation since the CH···O interaction does not occur along its major growth axis and is not critical for stabilizing its structure. The specific interaction with CBZ(M) and hydrogen-bond-accepting solvents leads to selective formation of CBZ(Trg) molecular motif, which allows nucleation of this polymorph to proceed.

CBZ(Trg) and CBZ(M) crystallized simultaneously in cyclohexane and hexanes. This observation is likely due to the inability for either solvent to hydrogen bond with CBZ molecules.

Chlorinated solvents exhibited similar behavior on CBZ nucleation as observed with acceptor solvents. The Cl atom may serve as an effective hydrogen bond acceptor.[37,43] A search of the Cambridge Crystallographic Database revealed that chlorinated solvents have a higher propensity to interact by accepting hydrogen bonds from C−H rather than from N−H functional groups (hydrogen-bond-donating groups present on CBZ molecule). In considering this finding, the C−H···Cl interaction between the CBZ dimers may prevent the C−H···O interactions that are critical for stabilizing the molecular motif of CBZ(M).

The effects of crystallizing solvent on sulfamerazine was thoroughly examined by Gu et al.[3] Gu et al. investigated the nucleation behavior and rate of solvent-mediated transformation of sulfamerazine from various organic solvents. The authors determined that the strength of the hydrogen bond was the important factor in inhibiting sulfamerazine nucleation. The nucleation rate was determined to be a function of the balance between solubility and strength of the solute−solvent interactions. The transformation from the metastable to the stable form of sulfamerazine was fastest in solvents with high solubilities and moderate solute−solvent interactions. The ability of a solvent to inhibit the nucleation of the stable form increased as the HBA propensity of the solvent increased. The ability of the solvent to strongly bind sulfamerazine molecules prevented the geometric requirements necessary for the stable form of sulfamerazine to nucleate. The results from their study show that the strength of the solute−solvent interaction and solubility were critical factors for directing polymorphic nucleation. In comparison, the strength of the CBZ−solvent hydrogen bond did not appear to be the main factor dictating its nucleation behavior. Rather, the ability of the solvent to donate and/or accept hydrogen bonds and the resulting effects on the CBZ crystal structures controlled CBZ nucleation behavior.

Conclusions

The present study shows that the hydrogen-bonding propensity of a solvent significantly affects nucleation outcomes and solvent-mediated transformations. Solvents with a propensity to accept hydrogen bonds inhibited CBZ(M) nucleation and delayed the CBZ(Trg) to CBZ(M) transformation, whereas solvents that are hydrogen bond acceptors and donors concomitantly crystallized both CBZ forms and facilitated the CBZ(Trg)-to-CBZ(M) transformation. CBZ−solvent interactions affect molecular associations that precede nucleation and interfere with the molecular motif for CBZ(M) formation. This study emphasizes the important role that hydrogen bonding and specific drug−solvent interactions have on facilitating or retarding the nucleation and growth of pharmaceutical polymorphs.

Acknowledgment

Financial support from the Horace Rackham School of Graduate Studies, University of Michigan, Fred W. Lyons Jr. Fellowship from the College of Pharmacy, University of Michigan, and the Purdue/Michigan Consortium on The Study of Supramolecular Assemblies and Solid-State Properties is acknowledged.

Received for review May 28, 2009.

OP900133Z

(39) Grzesiak, A. L.; Lang, M.; Kim, K.; Matzger, A. J. Comparison of the four anhydrous polymorphs of carbamazepine and the crystal structure of Form I. *J. Pharm. Sci.* **2003**, *92* (11), 2260–2271.

(40) Steiner, T. Unrolling the Hydrogen Bond Properties of C−H···O Interactions. *Chem. Commun.* **1997**, (8), 727–734.

(41) Steiner, T.; Desiraju, G. R. Distinction Between the Weak Hydrogen Bond and the Van Der Waals Interaction. *Chem. Commun.* **1998**, (8), 891–892.

(42) Desiraju, G. C−H···O and other weak hydrogen bonds. From crystal engineering to virtual screening. *Chem. Commun.* **2005**, (24), 2995–3001.

(43) Banerjee, R.; Desiraju, G.; Mondal, R.; Howard, J. Organic Chlorine as a Hydrogen-Bridge Acceptor: Evidence for the Existence of Intramolecular O−H···Cl−C Interactions in Some *gem*-Alkynols. *Chem.—Eur. J.* **2004**, *10* (14), 3373–3383.